Correlation effects in ferromagnetism of transition metals

A. M. Oleś* and G. Stollhoff
Max-Planck-Institut für Festkörperforschung, D-7000 Stuttgart 80, Federal Republic of Germany
(Received 17 September 1982; revised manuscript received 26 August 1983)

The effect of electronic correlations on the ferromagnetic instabilities, effective local moments, and fluctuations in spin and charge in a transition metal is discussed with a model Hamiltonian which includes intraatomic Coulomb and exchange interactions. The one-particle properties of d electrons are described by bcc and fcc canonical bands. We find that reduction of density fluctuations and formation of local moments change the Stoner criterion and the condition for the ground state to be completely ferromagnetic. The magnetic states of Fe, Co, and Ni are studied in more detail, where the electrons are found to be considerably correlated for realistic model parameters. Redistribution of electrons between the e_g and t_{2g} states seen there causes deviations from the Stoner theory and is responsible for different exchange splittings of both types of states. The results are in qualitative agreement with the experimental data and suggest the use of anisotropic exchange correlation potentials in transition metals.

I. INTRODUCTION

The treatment of d electrons in transition metals faces serious problems. On the one hand one knows from de Haas—van Alphen (dHvA), and magnetotransport experiments and from photoemission spectra that those electrons have to be described as delocalized band states. On the other hand, the Curie-type high-temperature magnetic susceptibility, existence of spin waves above T_c, or magnetic form factors rather indicate a localized atomlike behavior. This suggests that the d electrons, even when delocalized, have to be strongly correlated.

Attempts to treat those transition metals within the Hartree-Fock approximation (HFA) fail since the unphysically large charge fluctuations of the independent particles dominate the ground-state properties. The calculations within the local-spin-density functional (LSD) formalism allowed the elimination of that effect, because consequences of the charge fluctuations are avoided by the local treatment of the exchange. The success of that method concerning the calculation of magnetic moments[1] suggests that it should be able to treat total-energy differences between paramagnetic and ferromagnetic states with an accuracy better than 0.5 eV.

Being aware of the fact that those *ab initio* calculations lead to the best results which could be obtained up to now, we should also realize that there are some serious shortcomings connected with the approximations involved in calculations with a local exchange-correlation potential. Firstly, one cannot get information beyond the one-particle density such as pair correlation functions. Secondly, the LSD formalism mixes the effects of the Hund's-rule correlations, which are responsible for formation of atomiclike local moments with either the interaction of those local moments on different sites which may lead to a (anti)ferromagnetic ground state, or with a redistribution of electrons between different spin bands which leads to band ferromagnetism. All those effects are treated on an equal footing when going from a paramagnetic to a spin-split state within that formalism. The consequence is that energy differences between paramagnetic and ferromagnetic states are much too large as compared with Curie temperatures measured in transition metals.[2] In addition, within an LSD calculation the Stoner criterion, which is supposed to describe the onset of ferromagnetic ordering, might instead describe the creation of local moments on individual atoms only.

Finally, one knows that those calculations for Fe and Ni, for example, are not able to reproduce Fermi surface results very well. This implies that the one-particle density matrix in the ground state has not been determined properly. The error might result from the fact that one uses a local exchange-correlation potential which by its nature is not able to deal with anisotropic effects.

All those problems can be tackled only by treating the correlation of the d electrons explicitly. Since an *ab initio* calculation would be much too elaborate for the time being, we will study this problem with a simplified model Hamiltonian which consists of a tight-binding one-particle part for the d electrons and additionally some typical local interactions, described by Coulomb and exchange terms leading to a generalized Hubbard Hamiltonian.

Model calculations of this kind have been performed before for the paramagnetic state of transition metals. Two types of calculations were done. One applied a simplified rectangular density of states[3] for all five subbands while the other,[4] more elaborate, used the canonical bands of Andersen *et al.*[5] for the one-particle part of the energy. By comparing their results one obtains an understanding of how the details of the bands enter into the correlation calculation. It was shown that the correlation effects lead to the formation of local moments in accordance with Hund's rule. Furthermore, they reduce drastically the density fluctuations at an atomic site and enhance the spin fluctuations in the paramagnetic state. In particular it was found[4] that for band fillings of between 2 and 8 elec-

trons the energy gain due to formation of local moments is larger than 1000 K per atom when realistic parameters are used for the screened Coulomb and exchange interaction in 3*d* metals. Such strong correlations are expected to change the Stoner criterion and indeed the simplified model used in Ref. 3 indicates that this is the case.

The aim of the present investigation is to use the canonical *d* bands together with an extended Hubbard Hamiltonian in order to study in detail the correlations in the ferromagnetic phase and their effect on the Stoner criterion. The simpler Stoner theory[6] (ST) assumes that the *d* band splits as a whole into two spin subbands, so the energy of the ground state depends only on one Stoner parameter Δ. It is known, however, that the electronic interactions lead to different exchange potentials for different partial occupations. It has been shown, too, that the local correlation of electrons on the t_{2g} and e_g orbitals, is different depending on the given lattice symmetry. For instance, the e_g electrons are by about 50% stronger correlated than t_{2g} electrons in the bcc lattice and for about 7 electrons per atom.[4] Consequently, one also expects different magnetic moments localized on the e_g and t_{2g} orbitals than those resulting from the ST. Thus the energy of the ground state has to be minimized with respect to the magnetic moments in both t_{2g} and e_g orbitals, and also with respect to the possible change in their filling. Such a general formulation is reported and compared with ST in this paper. We also show how our theory leads to different exchange splittings (ES) for e_g and t_{2g} electrons, in qualitative agreement with the experiment, while the ST always gives the same ES for both types of electrons.

The energy of the ground state consists of the HFA part and the correlation energy. The latter was found within the local approach.[7,8] This method can be considered either as an extension of the Gutzwiller ansatz[9] or alternatively as an extension of the Jastrow method. It appeared to be very successful in calculations of molecules where it was able to reproduce 95% of the correlation energy within a given basis set.

The paper is organized as follows. The Hamiltonian and the method of calculation (the local approach) as well as the approximations involved are discussed in Sec. II. Section III contains a general discussion of the possible ferromagnetic instabilities of the system. The phase boundaries of the paramagnetic, weakly ferromagnetic, and completely ferromagnetic states are presented there for the bcc and fcc structures and compared with those resulting from the Hartree-Fock theory. Ferromagnetic ground states of 3*d* transition metals, Fe, Co, and Ni, are discussed in detail in Sec. IV. It is shown that the ground states are different to those predicted by the Stoner theory as the electrons shift between e_g and t_{2g} states with increasing interactions. The exchange splittings resulting from our model which show anisotropy between e_g and t_{2g} orbitals are also compared with the existing results of various theories and experiments. Furthermore some estimates for the ferromagnetic transition temperatures T_c are given. Conclusions and final remarks are given in Sec. V.

TABLE I. Exchange constants J_{ij} for *d* orbitals expressed by the average exchange interaction $J=\frac{1}{2}(J_{e_ge_g}+J_{t_{2g}t_{2g}})$ and the anisotropy $\Delta J=J_{e_ge_g}-J_{t_{2g}t_{2g}}$.

	zx	yz	xy	x^2-y^2	$3z^2-r^2$
zx	0	$J-\frac{1}{2}\Delta J$	$J-\frac{1}{2}\Delta J$	$J-\frac{1}{2}\Delta J$	$J-\frac{5}{2}\Delta J$
yz	$J-\frac{1}{2}\Delta J$	0	$J-\frac{1}{2}\Delta J$	$J-\frac{1}{2}\Delta J$	$J-\frac{5}{2}\Delta J$
xy	$J-\frac{1}{2}\Delta J$	$J-\frac{1}{2}\Delta J$	0	$J-\frac{7}{2}\Delta J$	$J+\frac{1}{2}\Delta J$
x^2-y^2	$J-\frac{1}{2}\Delta J$	$J-\frac{1}{2}\Delta J$	$J-\frac{7}{2}\Delta J$	0	$J+\frac{1}{2}\Delta J$
$3z^2-r^2$	$J-\frac{5}{2}\Delta J$	$J-\frac{5}{2}\Delta J$	$J+\frac{1}{2}\Delta J$	$J+\frac{1}{2}\Delta J$	0

II. LOCAL APPROACH TO CORRELATIONS IN TRANSITION METALS

The Hamiltonian used is similar to that in Ref. 4. Its one-particle part is the same and written in the tight-binding approximation. It describes a canonical *d* band[5,10,11] and contains one free parameter only, namely the bandwidth *W*. Furthermore, only interactions of electrons on the same atom are included, which are described by the Coulomb (U) and exchange (J) terms. The total Hamiltonian depends henceforth on three parameters and takes the form

$$H=H_0+H_1\ , \tag{2.1}$$

$$H_0=\sum_{\nu,\sigma,\vec{k}}\epsilon_\nu(\vec{k})n_{\nu\sigma}(\vec{k})\ , \tag{2.2}$$

$$H_1=\tfrac{1}{2}\sum_{\substack{l,i,j,\\ \sigma,\sigma'}}U_{ij}a^\dagger_{li\sigma}a^\dagger_{lj\sigma'}a_{lj\sigma'}a_{li\sigma} + \tfrac{1}{2}\sum_{\substack{l,i,j,\\ \sigma,\sigma'}}J_{ij}\{a^\dagger_{li\sigma}a^\dagger_{lj\sigma'}a_{li\sigma'}a_{lj\sigma}+a^\dagger_{li\sigma}a^\dagger_{li\sigma'}a_{lj\sigma'}a_{lj\sigma}\}\ . \tag{2.3}$$

$\epsilon_\nu(\vec{k})$ are the canonical band energies and $n_{\nu\sigma}(\vec{k})$ the corresponding number operators for the respective lattice geometry (i.e., bcc or fcc). The localized states i,j are the basis orbitals of the canonical bands adapted to cubic symmetry of e_g and t_{2g} type. They are represented by $a_{li\sigma}$, where l is the atomic site index, i,j the type of orbital, and σ the spin. (For more details about the one-particle properties see Ref. 12.) The matrix elements J_{ij} may be expressed by the exchange constant J and its anisotropy ΔJ, as presented in Table I. The Coulomb matrix elements have the following form:

$$U_{ij}=U+2J-2J_{ij}\ . \tag{2.4}$$

That interaction part H_1 is slightly different from the one in Refs. 3 and 4. It is the most general one allowed by the atomic symmetric[13] and has been used for transition metals before.[14] As in Ref. 14 we have chosen ΔJ to be $\Delta J=0.15J$ and are left with two independent parameters, namely U and J. If $\Delta J=0$, then this interaction part reduces to the one used in Ref. 15.

The *s* electrons are not included in the Hamiltonian (2.1) explicitly, so the hybridization effects are neglected. They are, however, implicitly taken into account by a

noninteger d-band occupation and a drastic screening of the otherwise very large Coulomb interaction U. Typical values for a bandwidth W are found in the LSD calculations,[11] while typical values of screened U and J were given by Friedel and Sayers.[16] The large reduction of U compared with a much smaller screening of J causes a relative increase in the anisotropy for the U_{ij}.

It is straightforward to calculate the ground state $|\psi_{\rm HF}\rangle$ of H_0 for different band occupancies n where n is an average electron filling per atom $0 \lesssim n \lesssim 10$. There are two kinds of information needed to perform the calculations presented below:

(1) local-density-matrix elements

$$P_{ij\sigma}^{ll} = \langle \Psi_{\rm HF} | a_{li\sigma}^{\dagger} a_{lj\sigma} | \Psi_{\rm HF} \rangle = \sum_{\substack{\vec{k} \in K(\sigma), \\ \nu}} d_{i\nu}^{*}(\vec{k}) d_{j\nu}(\vec{k}) = \delta_{ij} n_{i\sigma} , \tag{2.5}$$

which give the relative occupancies of e_g and t_{2g} states, and

(2) local-energy-matrix elements

$$E_{ij\sigma}^{ll} = \sum_{\substack{\vec{k} \in K(\sigma), \\ \nu}} d_{i\nu}^{*}(\vec{k}) d_{j\nu}(\vec{k}) \epsilon_{\nu}(\vec{k}) = \delta_{ij} f_{i\sigma} , \tag{2.6}$$

which give the mean kinetic energy per e_g and t_{2g} states in mean-field approximation. Summations in (2.5) and (2.6) run over the Bloch states filled with σ-spin electrons; $d_{i\nu}(\vec{k})$ determines the e_g or t_{2g} content of a Bloch state $(\vec{k},\nu,\sigma)$ and are given by $d_{i\nu}(\vec{k}) = \langle i | \vec{k},\nu \rangle$. $|\vec{k},\nu\rangle$ and $|i\rangle$ are the eigenvectors of the tight-binding matrix for a general $\vec{k}$ and for $\vec{k}=\vec{0}$ classified according to the cubic point group into e_g and t_{2g} states. The procedure to calculate them is analogous to the one used in Ref. 12.

Additionally one has

$$\sum_{i,\sigma} n_{i\sigma} = n , \tag{2.7}$$

$$\sum_{i,\sigma} f_{i\sigma} = \frac{1}{N} \langle \Psi_{\rm HF} | H_0 | \Psi_{\rm HF} \rangle . \tag{2.8}$$

Let us point out that the one-particle density matrix of the actual ground state is generally not the one of H_0. Instead it is modified due to spin splitting as concerns a magnetic state, and due to the mean-field part as well as the correlation effects originating from H_1. To include these effects one would in principle have to repeat those calculations with pseudo crystal fields $g_{i\sigma}$:

$$H'_{0\sigma} = H_{0\sigma} + \sum_{l,i} g_{i\sigma} a_{li\sigma}^{\dagger} a_{li\sigma} , \tag{2.9}$$

for which

$$g_{i\sigma} = \begin{cases} 3a_{\sigma} & \text{for } i \in e_g , \\ -2a_{\sigma} & \text{for } i \in t_{2g} , \end{cases} \tag{2.10}$$

which would modify the elements $f_{i\sigma}$,

$$f_{i\sigma} \rightarrow f'_{i\sigma}(\{n_{i\sigma}\}) . \tag{2.11}$$

However, in order to simplify the numerical procedure we have approximated them by the paramagnetic ones. This approximation is expected to cause only small quantitative changes in the results and should be reasonable as long as the redistribution of electrons within the spin subbands is small.

The correlations are treated within the local approach (LA) (Refs. 7 and 8) which describes a correlated ground state $|\Psi_L\rangle$ by the respective modifications of the HF ground state,

$$|\Psi_L\rangle = \prod_{l,n} (1 - \eta_n O_{ln}) |\Psi_{\rm HF}\rangle . \tag{2.12}$$

Here we choose operators O_{ln} of the form

$$\begin{aligned} O_{li}^{(1)} &= n_{li\uparrow} n_{li\downarrow} , \\ O_{lij}^{(2)} &= n_{li} n_{lj} , \quad i \neq j \\ O_{lij}^{(3)} &= \vec{S}_{li} \cdot \vec{S}_{lj} , \quad i \neq j . \end{aligned} \tag{2.13}$$

This ansatz allows the reduction of charge fluctuations on each atom by $O_{li}^{(1)}$ within one and by $O_{lij}^{(2)}$ between different states. Spin correlations which lead to formation of local moments are described by $O_{lij}^{(3)}$. For conveniences the modification of the Hartree-Fock state $|\Psi_{\rm HF}\rangle$ is chosen to be orthogonal to $|\Psi_{\rm HF}\rangle$, so $\langle O_{ln} \rangle_{\rm HF} = 0$ and no contractions within the operators $\{O_{ln}\}$ are allowed. It corresponds to taking only connected diagrams in the expansion of the ground-state energy.[17] Therefore the factors $(1 - \eta_n O_{ln})$ are not projection operators as in the Gutzwiller method,[9] but the meaning of $\{O_{ln}\}$ is similar. This point has also been discussed elsewhere.[4,8]

The parameters η_n are determined by minimization of the ground-state energy, normalized per site

$$E_L = \frac{\langle \Psi_L | H | \Psi_L \rangle}{N \langle \Psi_l | \Psi_L \rangle} = E_{\rm HF} + \Delta E_L . \tag{2.14}$$

The correlation energy ΔE_L is calculated within two approximations. The first is to expand energies in powers of η_n and keep terms only up to η_n^2; the second is to treat the correlations on different sites as independent of each other. The latter step corresponds to a local cluster approximation. In second-order-perturbation expansion calculations for the correlation energy it was also called the $\vec{R}=0$ approximation.[18] The result for ΔE_L is

$$\begin{aligned} \Delta E_L &= -2 \sum_{n} \eta_n \langle O_{ln} \tilde{H} \rangle + \sum_{n,n'} \eta_n \eta_{n'} \langle O_{ln} \tilde{H} O_{ln'} \rangle \\ &= - \sum_{n,n'} \langle O_{ln} \tilde{H} \rangle \{ \langle O_{lm} \tilde{H} O_{lm'} \rangle \}_{nn'}^{-1} \langle O_{ln'} \tilde{H} \rangle \end{aligned} \tag{2.15}$$

with

$$\tilde{H} = H - \langle H \rangle . \tag{2.16}$$

Both approximations mentioned above have been checked in the paramagnetic case.[4] It has been found that the first one, the variational expansion up to η_n^2 gives satisfactory results (contrary to second-order-perturbation expansion) for realistic values of the parameters U/W and J/W and

may be used as long as $U < W$. The second approximation modifies the results for the correlation energies and the parameters η_n by less than 5%.

Owing to both approximations there are only relatively few matrix elements $\langle O_{ln}\tilde{H}\rangle$ and $\langle O_{ln}\tilde{H}O_{ln'}\rangle$ which have to be calculated. The detailed form of these matrix elements, which are dependent only on $n_{i\sigma}$ and $f_{i\sigma'}$ is given in Appendix A. They had to be generalized to ferromagnetic states from Ref. 4 and to different orbital states from the model of equivalent bands.[3]

The HF energy $E_{\rm HF}$ consists of the kinetic energy $E_{\rm kin}$ and the mean-field part of the interaction energy $E_{\rm MF}$,

$$E_{\rm HF}=E_{\rm kin}+E_{\rm MF}\ , \tag{2.17}$$

where

$$E_{\rm kin}=\sum_{i\sigma} f_{i\sigma}\ , \tag{2.18}$$

$$E_{\rm MF}=\sum_i U_{ii}n_{i\uparrow}n_{i\downarrow} + \sum_{\substack{i,l,j,\\ \sigma,i\neq j}} \{U_{ij}n_{i\sigma}n_{j-\sigma}+(U_{ij}-J_{ij})n_{i\sigma}n_{j\sigma}\}\ . \tag{2.19}$$

The total energy is now minimized as a function of the electron occupations $n_{i\sigma}$ with the constraint (2.6). Results of such calculations for bcc and fcc lattices performed in both Hartree-Fock and local approximations are reported in Sec. III.

III. FERROMAGNETIC INSTABILITIES IN THE CANONICAL BANDS

The local interactions of the Hamiltonian (2.1)—(2.3) lead to changes in the local occupations $n_{i\sigma}$ of different orbitals compared with the noninteracting ground state.

One kind of redistribution is present in the paramagnetic state, namely a redistribution of t_{2g} and e_g occupations. It is represented by

$$\Delta n_{t_{2g}}=\sum_\sigma (n_{t_{2g}\sigma}-n^{(0)}_{t_{2g}\sigma}) \tag{3.1}$$

where $n^{(0)}_{t_{2g}}$ stands for the filling of t_{2g} states without interaction.

In HFA, for example, the difference of the e_g Fermi level (μ_e) and the t_{2g} level (μ_t),

$$\Delta_p=\mu_t-\mu_e\ , \tag{3.2}$$

can be taken as the measure of electron redistribution instead of $\Delta n_{t_{2g}}$. Differentiating $E_{\rm HF}$ with respect to Δ_p and obeying (2.6) one obtains

$$\frac{\partial E_{\rm HF}}{\partial \Delta_p}=[2\Delta_p-(U-3J+\tfrac{35}{2}\Delta J)(n_t-n_e)] \times[3D_t(\mu_t)+2D_e(\mu_e)]=0\ . \tag{3.3}$$

Here D_t and D_e are the t_{2g} and e_g densities of state, respectively. Equation (3.6) shows that one always has a redistribution with the exception of equal filling $n_t=n_e$. The subband with larger occupation adsorbs additional electrons in order to reduce the mean-field part of the interaction energy. It will be shown that those redistributions are rather small and further reduce in the correlated case.

The two other kinds of redistributions are directly connected with the ferromagnetic state. They cause the creation of magnetic moments for e_g and t_{2g} subbands,

$$m_i=n_{i\uparrow}-n_{i\downarrow}\ . \tag{3.4}$$

Those magnetic moments can be represented by exchange splittings (Δ_i, $i=e_g$, t_{2g}) which are the differences in the Fermi levels

$$\Delta_i=\mu_{i\uparrow}-\mu_{i\downarrow}\ . \tag{3.5}$$

The three splittings as given in (3.1) and (3.5) define the ground state of the Hamiltonian (2.1)—(2.3). They are a generalization of the single exchange splitting Δ from ST (Ref. 6) as discussed by Thalmeier and Falicov.[12]

Knowing the optimal paramagnetic state (and Δ_p) we can now look at the ferromagnetic instability given by

$$\begin{vmatrix} \frac{\partial^2 E}{\partial \Delta_t^2} & \frac{\partial^2 E}{\partial \Delta_t \partial \Delta_e} \\ \frac{\partial^2 E}{\partial \Delta_t \partial \Delta_e} & \frac{\partial^2 E}{\partial \Delta_e^2} \end{vmatrix}=0\ . \tag{3.6}$$

This criterion replaces the Stoner criterion for a single exchange splitting. In one-particle approximation it can be received analytically to be

$$[1-(U+4J-\Delta J)D_t(\mu_t)][1-(U+3J+\tfrac{1}{2}\Delta J)D_e(\mu_e)] -6(J-\tfrac{3}{2}\Delta J)^2 D_e(\mu_e)D_t(\mu_t)=0\ . \tag{3.7}$$

That instability appears simultaneously in both subbands. Equation (3.7) is fulfilled for a smaller value of U than any of the conditions

$$(U+3J+\tfrac{1}{2}\Delta J)D_e(\mu_e)=1\ ,$$
$$(U+4J-\Delta J)D_t(\mu_t)=1\ , \tag{3.8}$$

which lead to a Stoner instability in one of the subbands only. In the case $J=0$, (3.7) is equivalent to (3.8); both subbands are then decoupled.

The condition for a Stoner instability is

$$3(U+J+\tfrac{19}{2}\Delta J)\frac{D_t^2(\mu)}{D(\mu)}+2(U+J+\tfrac{7}{2}\Delta J)\frac{D_e^2(\mu)}{D(\mu)} +(J-\tfrac{3}{2}\Delta J)D(\mu)=1\ ,$$

where

$$D(\mu)=3D_t(\mu)+2D_e(\mu)\ . \tag{3.9}$$

For the model of five equivalent subbands of Friedel and Sayers (3.7) and (3.9) reduce to the same condition

$W=U+6J$.[3] The correlated case can only be treated numerically.

The instability of the completely ferromagnetic (CF) state with respect to the weakly ferromagnetic (WF) state may be studied in the same manner. CF means that one set of spin subbands is either completely filled ($n \geq 5$) or empty ($n \leq 5$). Having found the optimal CF state (i.e., the distribution in between e_g and t_{2g} bands) one can see whether

$$\left.\frac{\partial E}{\partial \Delta_i}\right|_{\mathrm{CF}} \geq 0 . \tag{3.10}$$

For the one-particle approximation one obtains

$$\begin{aligned} \Delta_t &\geq (U+4J-\Delta J)m_t+2(J-\tfrac{3}{2}\Delta J)m_e , \\ \Delta_e &\geq (U+3J+\tfrac{1}{2}\Delta J)m_e+3(J-\tfrac{3}{2}\Delta J)m_t . \end{aligned} \tag{3.11}$$

If both conditions (3.10) become fulfilled before (3.6) then the CF state is either stable or metastable if compared with the paramagnetic state.

The ferromagnetic instabilities are analyzed in three successive approximations. Firstly, the generalized Stoner criterion within the HFA is treated, i.e., without correlation effects. Secondly, only density correlations are included in the calculation of the correlation energy ΔE_L. This approximation simulates qualitatively the LSD theory working with a local correlation potential. Finally, spin correlations are also included to test how such modified Stoner criteria depend on the creation of local moments.

Figure 1 shows the phase diagram of the bcc lattice obtained with $J/U=0.2$. This ratio of the exchange interaction to the Coulomb interaction is realistic for transition metals[16] and was accepted by us for most of the presented calculations. The lower part of the figure shows the criterion for the instability of WF states [Fig. 1(b)], the upper the instability for CF states [Fig. 1(a)]. The lowest curves in each part are obtained within the HFA. The structure seen in this criterion [Fig. 1(b)] is directly connected with the canonical density of states for the bcc lattice. The middle curve in Fig. 1(b) shows that density correlations shift that criterion rather homogeneously, except for small fillings ($n \simeq 0$, or 10), when substantially stronger interactions are needed to obtain ferromagnetic states. The spin correlations behave similarly for the WF transition. They show stronger dependence on the actual ratio U/W nevertheless.

Figure 1(a) shows the criterion for complete ferromagnetism. Again, the density correlations shift those transitions rather consistently to larger interactions, while the spin correlations add a completely new structure, excluding complete ferromagnetism in the regions $2.5<n<4.7$ and $5.8<n<6.5$ for realistic values of model parameters.

Figure 2 shows the ferromagnetic instabilities for the fcc case with $J/U=0.2$. Density correlations again shift the critical interactions rather consistently towards larger values while spin correlations depend strongly on the size of U/W. Altogether, complete ferromagnetism seems to be excluded for $U/W<0.8$ and $n<4.5$.

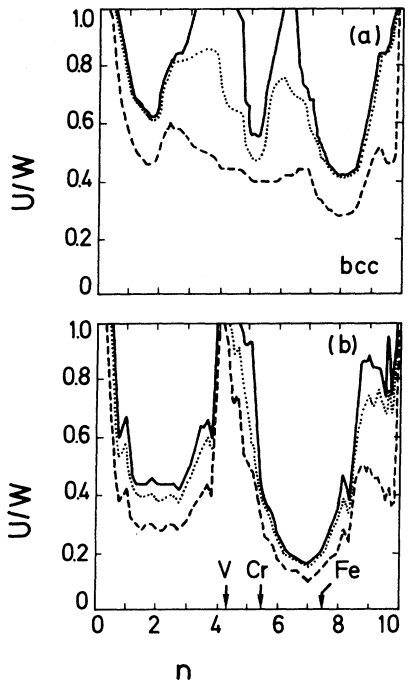

FIG. 1. Ferromagnetic instabilities with respect to formation of (a) CF and (b) WF states for the bcc lattice obtained with $J/U=0.2$. Broken lines, dotted lines, and continuous lines stand for HF, LA without spin-spin correlations, and LA with spin-spin correlations.

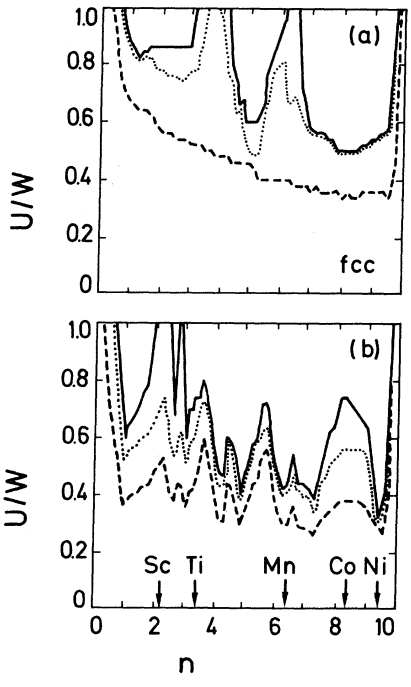

FIG. 2. The same as in Fig. 1 for the fcc lattice.

TABLE II. Critical values of the ratio U/W with respect to formation of weak (WF) and complete (CF) ferromagnetism for the electron fillings n corresponding to 3d transition metals and different ratios J/U.

	Cr (bcc, $n=5.4$)		Mn (fcc, $n=6.3$)		Fe (bcc, $n=7.4$)		Co (fcc, $n=8.3$)		Ni (fcc, $n=9.4$)	
J/U	WF	CF	WF	CF	WF	CF	WF	CF	WF	CF
0	1.47	1.02	1.25	>2	0.48	1.32	1.12	0.95	0.65	0.95
0.1	0.66	0.78	0.62	1.11	0.29	0.70	0.85	0.64	0.40	0.69
0.2	0.45	0.63	0.43	1.02	0.20	0.48	0.71	0.47	0.25	0.56
0.3	0.35	0.52	0.32	0.85	0.15	0.36	0.62	0.39	0.19	0.47

Arrows in both figures indicate band fillings in that model corresponding to real substances in 3d series. They are taken from Ref. 19. Firstly it can be seen in Fig. 1 that the criterion of WF for Fe is almost unchanged by spin correlations and predicts a critical $U/W=0.2$. Cr lies in a region of drastic changes of the ferromagnetic instability, so approximations for the one-particle band structure might be important. One can expect the paramagnetic state to be stable up to $U/W\simeq 0.45$. V lies in a region without steady transition; its paramagnetic state remains stable up to $U/W\sim 1.0$. In Fig. 2 we see that spin correlations almost do not influence the ferromagnetic transitions of Ni, while for Co the paramagnetic state becomes metastable in a certain parameter range. Mn is certainly paramagnetic for $U/W<0.5$.

Figures 1 and 2 were obtained for $J/U=0.2$, the ratio considered to be realistic for transition metals.[16] Table II gives some representative values of the critical U/W for $J/U=0$ up to 0.3. They can be seen to depend stronger on J than it is suggested by the scaling relation $W=U_c+6J_c$, which was found in the degenerate band case.[3,15]

Concluding, it can be said that spin correlations substantially influence phase transitions to ferromagnetic states in the region close to the half-filled bands.

IV. FERROMAGNETIC STATES OF 3d TRANSITION METALS

Having described general trends for the series of transition metals within the last chapter, we will deal in this part with three special cases: Fe (bcc), Co and Ni (fcc), and discuss their ground-state properties.

Fe is described by the Hamiltonian (2.1)—(2.3) with a total number of 7.4 electrons per atom. Table III lists some characteristic energy differences for Fe. One can see that the energy gain due to a ferromagnetic transition is reduced from ~ 0.56 eV within HFA (ΔE_{HFA}) to ~ 0.15 eV when the correlated states are compared (ΔE_{LA}). That amount increases by a factor of 1.5 to 0.22 eV ($\Delta E^{1}_{\mathrm{LA}}$) when local spin correlations are neglected for the paramagnetic and ferromagnetic case. The difference between $\Delta E^{1}_{\mathrm{LA}}$ and ΔE_{LA} compares rather well with the energy gained by spin correlations in the paramagnetic phase[4] ($\Delta E^{\mathrm{LM}}_{\mathrm{LA}}$). This demonstrates that the almost complete band ferromagnetic phase contains all local spin correlations.

Figure 3 shows how the diagonal one-particle matrix elements change for the ground state, depending on U/W (with $J/U=0.2$). The upper part gives the results of HFA, the lower of LA. It can be seen how the occupancies of local states change depending on the spin index. The spin splitting begins for $U/W=0.20$ (0.15 in HFA) and the e_g majority band is filled at 0.38 (0.32 in HFA). Finally, the system becomes completely ferromagnetic for $U/W=0.48$ (0.34 in HFA). The experimental value of the magnetic moment $2.2\mu_B$ was found with $U/W=0.44$ (0.31 in HFA). In that region the moment depends strongly on U; its change by 5% would lead to a change of the moment by 15%.

Figure 3 shows also how charge transfers from e_g to t_{2g} states. The dotted lines represent what happens in ST, i.e., if the spin bands are shifted against each other. The additional adjustment allowed by the procedure given above leads to a transfer presented by the broken lines. One can see that in the HFA the system tries to reduce the charge fluctuations by an artificial redistribution of electrons. This effect is missing in the LA. There is, however, still a larger charge transfer from minority e_g states to minority t_{2g} states than that given by ST. This can be understood as anisotropic spin splitting—the e_g states split more than the t_{2g} states. The reason might be that the e_g states con-

TABLE III. Energy differences (in eV) between the paramagnetic and ferromagnetic states of Fe [bcc, $n=7.4$, $W=5.43$ eV (Ref. 11)] obtained in HFA (ΔE_{HFA}), LA (ΔE_{LA}) and the LA without spin correlations ($\Delta E^{1}_{\mathrm{LA}}$) for different values of U and J (in eV). $\Delta E^{\mathrm{LM}}_{\mathrm{LA}}$ stands for the energy gain in the paramagnetic states due to formation of local moments.

J/U	U	J	$\langle S^z\rangle$	ΔE_{HFA}	ΔE_{LA}	$\Delta E^{1}_{\mathrm{LA}}$	$\Delta E^{\mathrm{LM}}_{\mathrm{LA}}$
0.2	2.281	0.456	1.88	0.451	0.128	0.190	0.066
	2.389	0.478	2.12	0.564	0.150	0.221	0.074
	2.444	0.489	2.36	0.676	0.163	0.242	0.079
0.3	1.738	0.521	2.12	0.469	0.117	0.197	0.087
	1.846	0.554	2.36	0.607	0.147	0.246	0.101
	1.901	0.570	2.60	0.723	0.163	0.271	0.108

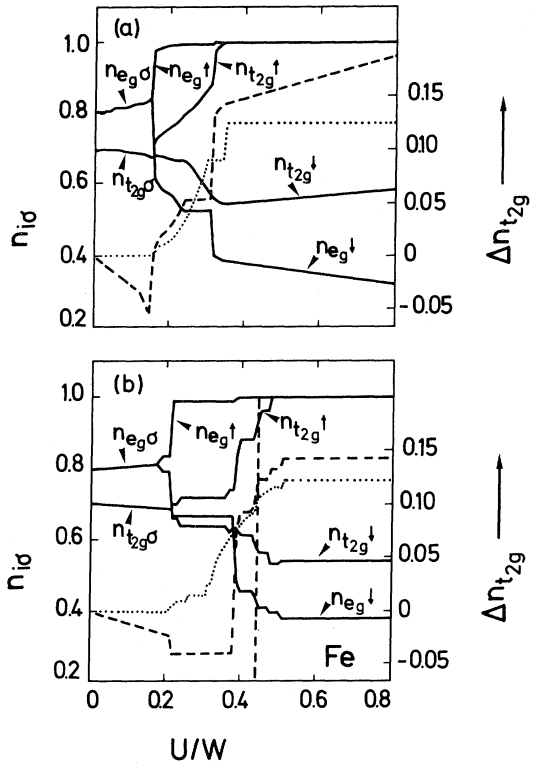

FIG. 3. Electron fillings $n_{i\sigma}$ (continuous lines) of e_g and t_{2g} states for different values of U/W obtained in (a) HFA and (b) LA for Fe. Broken lines represent $\Delta n_{t_{2g}}$ in the present calculation; dotted lines $\Delta n_{t_{2g}}$ in the Stoner theory. Values of $n_{i\sigma}$ corresponding to the magnetic moment $2.2\mu_B$ are indicated in (b) by the vertical broken line. Parameters: bcc lattice, $J/U=0.2$, $n=7.4$.

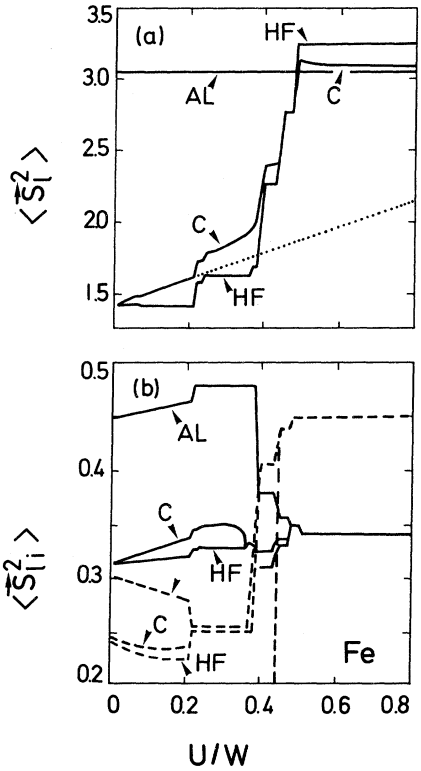

FIG. 4. Local moments (a) total $\langle \vec{S}_l^2 \rangle$ and (b) on different orbitals $\langle \vec{S}_{li}^2 \rangle$ (solid lines for t_{2g}, broken lines for e_g) per site in the ground state of Fe. HF, C, and AL stand for the results of the Hartree-Fock approximation, local approach and atomic limit, respectively. Parameters are the same as in Fig. 3. Dotted line in (a) corresponds to the paramagnetic state.

tain more holes. It has been shown before for the paramagnetic case that the e_g electrons correlate more strongly than the t_{2g} ones,[4] which was suspected to lead to anisotropic exchange-correlation potentials. The above mentioned result additionally supports that conjecture. Such a redistribution has not been found in LSD calculations.

To get more insight into the properties of ground states of the respective transition metals, we have calculated also local moments $\langle \vec{S}_l^2 \rangle$ per site, $\langle \vec{S}_{li}^2 \rangle$ per site and orbital, as well as charge and spin fluctuations, $\sigma^2(n_l)$ and $\sigma^2(S_l^z)$, defined in a standard way,

$$\sigma^2(nl)=\langle n_l^2 \rangle - \langle n_l \rangle^2 , \tag{4.1}$$

$$\sigma^2(S_l^z)=\langle (S_l^z)^2 \rangle - \langle S_l^z \rangle^2 . \tag{4.2}$$

Details of the calculation are given in Appendix B.

Figure 4 shows the local spin-correlation functions for Fe. For the expectation value of the square of the local moment $\langle \vec{S}_l^2 \rangle$ the following limiting values can be given: firstly the atomic limit (AL) within the same distribution of electrons in e_g and t_{2g} states as for $U=0$, and secondly the HFA limit of the CF state which has to be above the AL due to density fluctuations within single orbitals present in the HFA state. The curve C shows $\langle \vec{S}_l^2 \rangle$ for the correlated ground state. It can be seen how the electrons correlate within the paramagnetic state ($U/W<0.2$). The ferromagnetic state drives then the value of $\langle \vec{S}_l^2 \rangle$ above the AL. Finally that value converges slowly to the AL. For comparison, the local moment of a HF state, calculated with the same one-particle density matrix (that is, not the HF ground state), is given. It converges to the HFA limit.

The lower part of Fig. 4 plots the local moments for e_g and t_{2g} subbands $\langle \vec{S}_{li}^2 \rangle$. Here again the values obtained in the correlated ground state are compared with the HFA and the AL. It can be seen that correlations are not very strong before the system becomes completely ferromagnetic. Crossing of the values corresponding to both orbitals is due to a shift in electron filling, as displayed in Fig. 3.

Figure 5 shows the reduction of the density fluctuations in the correlated as well as in the HFA states. It can be seen that the onset of ferromagnetism almost plays no role for that value. This result is understandable since charge fluctuations are connected with energies which are by an order of magnitude larger than those connected with spin ordering. The spin fluctuations (Fig. 5) necessarily increase at the beginning for the paramagnetic state which has no preferred direction of magnetization; then they decline rather sharply and have the same limiting behavior

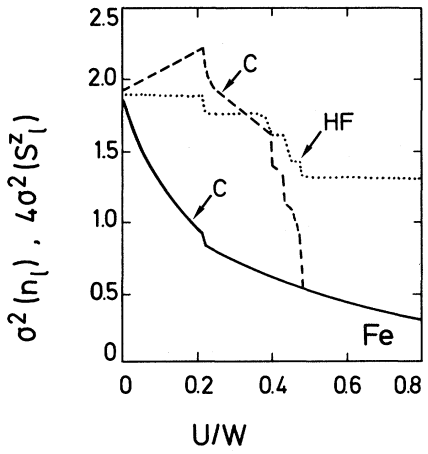

FIG. 5. Charge (solid line) and spin (broken line) fluctuations in the correlated ground state (C) for bcc Fe ($J/U=0.2$, $n=7.4$). HF stands for the HFA for both quantities.

within the completely ferromagnetic case as the density fluctuations. There they differ only by a prefactor. In the HFA the spin and charge fluctuations are proportional to each other, also in the paramagnetic and weakly magnetic states.

The second ferromagnetic transition metal which we want to discuss is Co (fcc), described by the Hamiltonian (2.1)—(2.3) with $n=8.3$. Table IV gives analogous energy differences to those already analyzed for Fe, found for different parameter sets. Based on the results of the recent LSD calculations, we have assumed the bandwidth $W=4.84$ eV.[11] Experiments indicate that the ground state has to be completely ferromagnetic, so only a lower limit for the interaction parameters U/W can be given. It decreases with increasing value of the ratio J/W. We see in Table III that the energy gain due to ferromagnetic ordering is larger by a factor of 3—5 in the HFA (ΔE_{HFA}) than in the correlated ground state (ΔE_{LA}). The latter is roughly 0.11 eV and typically equal to or up to two times larger than the energy gain due to local moments in the paramagnetic state ($\Delta E_{\mathrm{LA}}^{\mathrm{LM}}$). Not allowing for local moment formation would thus increase the energy difference for ferromagnetic ordering by up to a factor of 2 (to $\Delta E_{\mathrm{LA}}^{1}$).

Figure 6 shows the diagonal one-particle density matrix elements for e_g and t_{2g} majority and minority states. It can be seen that within the HFA [Fig. 6(a)] the transition to the CF state is rapid and takes place at $U/W=0.37$ being simultaneously connected with a large redistribution of electrons. For the correlated state this transition is also discontinuous at $U/W=0.55$. Owing to correlation effects there is a charge redistribution taking place already for the paramagnetic state and proceeding to rather large values within the ferromagnetic state. As for Fe, we find in Co more holes within e_g ferromagnetic states than in the ST.

TABLE IV. The same as in Table III for Co [fcc, $n=8.3$, $W=4.84$ eV (Ref. 11)].

J/U	U	J	ΔE_{HFA}	ΔE_{LA}	$\Delta E_{\mathrm{LA}}^{1}$	$\Delta E_{\mathrm{LA}}^{\mathrm{LM}}$
0.2	2.904	0.581	0.356	0.067	0.108	0.041
	3.146	0.629	0.430	0.113	0.161	0.048
	3.388	0.678	0.507	0.158	0.215	0.056
0.3	2.420	0.726	0.400	0.075	0.144	0.069
	2.662	0.799	0.493	0.123	0.208	0.084
	2.904	0.871	0.587	0.171	0.273	0.102

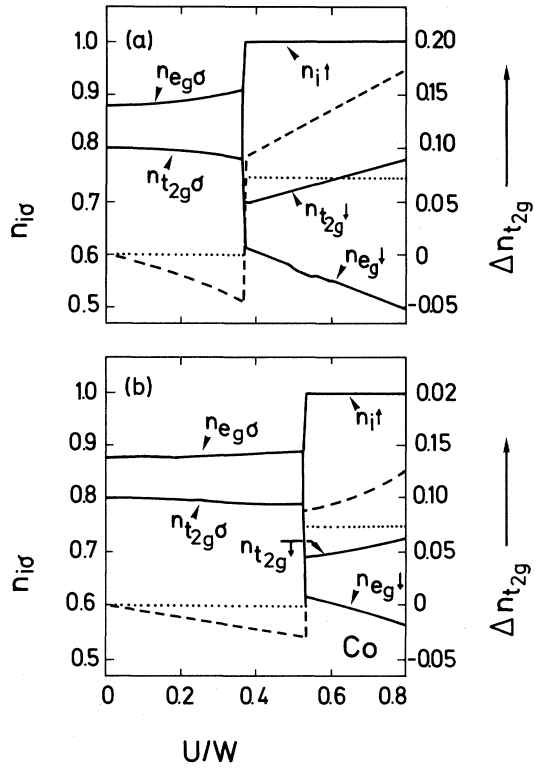

FIG. 6. The same as in Fig. 3 but for Co. Parameters: fcc lattice, $J/U=0.2$, $n=8.3$.

Formation of local moments in Co is presented in Fig. 7. The total moment per site $\langle \vec{S}_I^2 \rangle$ is compared with the HF and AL values in Fig. 7(a). Already in the paramagnetic state we can observe its formation; in the ferromagnetic state ($U/W>0.54$) the asymptotic approach towards the AL can be seen. The lower part [Fig. 7(b)] shows the diagonal matrix elements $\langle \vec{S}_{Ii}^2 \rangle$. It can be seen that the electrons are not too strongly correlated within single states before the system becomes completely ferromagnetic.

Finally, the results for Ni (fcc) are given. They were obtained with $n=9.4$ electrons/atom and $W=4.35$ eV.[11] Table V contains energy differences analogous to those discussed already for Fe and Co. The energy gain due to ferromagnetic ordering (ΔE_{LA}) is again reduced by about three times as compared with the HFA (ΔE_{HFA}), being basically rather low, namely smaller than 500 K. The spin correlations are not of great importance here and their neglectance would increase the respective energy difference ($\Delta E_{\mathrm{LA}}^{1}$) only by 10—20%. The absolute value of the respective energy gain ($\Delta E_{\mathrm{LA}}^{\mathrm{LM}}$) is less than 100 K, so they should have almost no effect in the thermodynamically interesting regions.

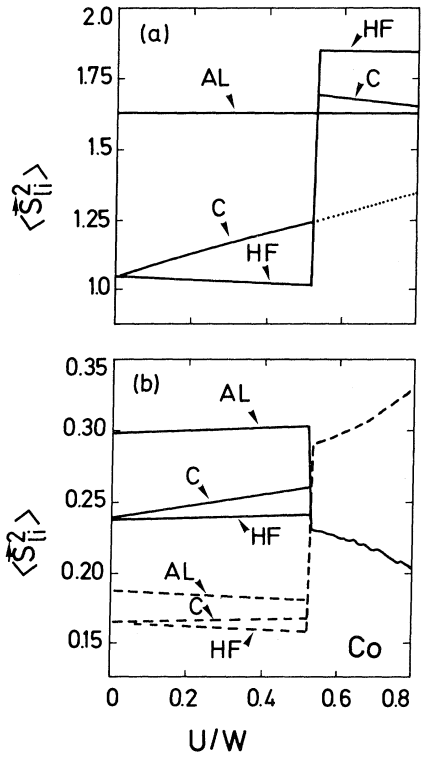

FIG. 7. The same as in Fig. 4 but for Co. Parameters are the same as in Fig. 6.

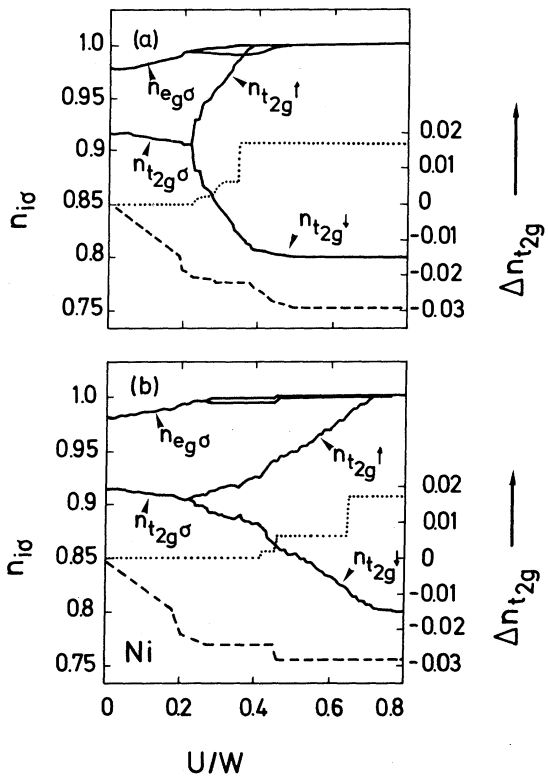

FIG. 8. The same as in Fig. 3 but for Ni. Parameters: fcc lattice, $J/U=0.2$, $n=9.4$.

Figure 8 shows the diagonal density-matrix elements within the HFA [Fig. 8(a)] and for the correlated state [Fig. 8(b)]. The Stoner criterion is modified by the correlation effects (from $U/W=0.22$ to 0.25) and the complete magnetization is reached in the HFA state at $U/W=0.39$ compared with 0.72 in the correlated case. Thus in order to describe Ni we have to assume $U/W>0.72$ since the d states in ferromagnetic Ni are completely spin-polarized. The charge redistribution between e_g and t_{2g} states is due to density fluctuations which tend to be decreased by filling e_g states, which contain more electrons in the paramagnetic state than the t_{2g} states. Contrary to Fe and Co, the minority band of e_g is here more filled than the t_{2g} band, so that one can connect the anisotropic effects seen in the ferromagnetic state with anisotropic populations of e_g and t_{2g} states. This shift is missing in LSD calculations again.

Interpretation of Fig. 9, which gives the values of local moments in Ni, is similar to that of Fig. 7. However, due to a relatively small number of holes, they have little possibility to correlate according to Hund's rule as well as within single states.

Above redistributions of one-particle densities have been discussed as they are received directly from ground-state calculations. In addition one can match those modifications into effective one-particle exchange potentials Δ_{e_g} and $\Delta_{t_{2g}}$. They are defined as leading to the exact one-particle density when added to the one-particle Hamiltonian (2.2). Those terms can be compared directly with the exchange splitting found from ST (Ref. 6) or LSD calculations.[11,20] The same exchange potentials have been used on the other hand to fit a similar kinetic Hamiltonian to experimentally known magnetic moments.[21]

Here the values 5.43 eV, 4.84, and 4.35 eV are taken for W of Fe, Co, and Ni from LSD calculations.[11] Accepting for the ratio of exchange to Coulomb interaction a value

TABLE V. The same as in Table III for Ni [fcc, $n=9.4$, $W=4.35$ eV (Ref. 11)].

J/U	U	J	ΔE_{HFA}	ΔE_{LA}	$\Delta E_{\mathrm{LA}}^{1}$	$\Delta E_{\mathrm{LA}}^{\mathrm{LM}}$
0.2	3.045	0.609	0.097	0.028	0.032	0.003
	3.263	0.653	0.115	0.035	0.039	0.003
	3.480	0.696	0.129	0.042	0.046	0.004
	3.698	0.740	0.142	0.050	0.054	0.004
0.3	2.828	0.566	0.120	0.031	0.037	0.006
	3.045	0.609	0.137	0.038	0.045	0.007
	3.263	0.653	0.152	0.044	0.052	0.007
	3.480	0.696	0.168	0.051	0.060	0.009

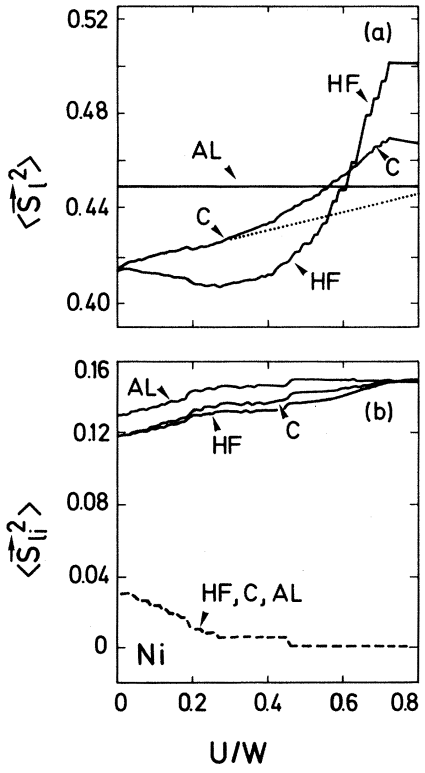

FIG. 9. The same as in Fig. 4 but for Ni. Parameters the same as in Fig. 8.

of $J/U=0.2$, and knowing the magnetic moments of 2.2, 1.6, and $0.6\mu_B$ for Fe, Co, and Ni one finds a Coulomb interaction of 2.4, $\gtrsim$2.6, and $\gtrsim$3.1 eV, respectively.

Here for Co and Ni the values of 3.1, and 3.3 eV have been chosen. In addition it has been assumed that the completely filled energy band ends just at the Fermi energy.

Those values of U are by a factor of 1.5–2 larger than the ones found by a recent calculation of Treglia *et al.*[22] who included many-body effects by second-order-perturbation expansion only. It is well known from the paramagnetic calculations[4] that for the actual range of interactions a second-order-perturbation expansion leads to results which are generally by a factor of 3 too large. In order to get results which might favorably compare with experiments the authors[22] therefore had to choose unphysically small interactions.

However, our ratio of $U/W=0.44$, 0.65, and 0.75 for Fe, Co, and Ni, agrees rather well with the earlier calculation of Cox *et al.*[23] who obtained $U/W=0.48$, 0.58, and 0.72, respectively.

In the case of Fe it turns out that $\Delta_{e_g}=1.74$ eV and $\Delta_{t_{2g}}=1.30$ eV. It compares well with a mean Δ of 1.55 eV (Refs. 1 and 24) or 1.97 eV (Ref. 11) from LSD calculations and with Δ of 1.45 eV from photoemission.[25] It should be realized, though, that there is no direct connection to quasiparticle properties. Trends should nevertheless be given qualitatively correct. The fitting procedure of Cooke *et al.*[21] on the other hand gave a uniform shift of $\Delta_{e_g}=\Delta_{t_{2g}}=2.2$ eV in that case. It cannot be concluded yet whether the failure of LSD calculations for the Fermi surface, especially around the N point,[24] can be connected with this anisotropy. It has been found, though, that an empirical anisotropic potential when added improves LSD calculations and fits dHvA measurements much better.[24]

In the case of Co, exchange splittings of $\Delta_{e_g}=1.28$ eV, $\Delta_{t_{2g}}=1.06$ eV have been received. LSD calculations vary in between 1.49 (Ref. 11) and 1.72 eV;[24] the experimental value is 1.10 eV.[25]

For Ni, rather strongly anisotropic splittings have been obtained, $\Delta_{e_g}=0.15$ eV, $\Delta_{t_{2g}}=0.57$ eV. Contrary to Fe and Co, that strong anisotropy is partially caused by the differences in U_{ij} and J_{ij} due to the term ΔJ. If $\Delta J=0$ it decreases somewhat to $\Delta_{e_g}=0.27$ and $\Delta_{t_{2g}}=0.50$ eV. LSD calculations received isotropic splittings of between 0.6 (Ref. 11) and 0.65 eV,[24] which were much larger. The anisotropy found here corresponds very well to the one of Ref. 21 where $\Delta_{e_g}\simeq 0.1$ and $\Delta_{t_{2g}}\simeq 0.4$ eV. Experimental mean-exchange splittings are given as 0.31,[25] 0.42,[26] and 0.27 eV.[27] Many-body calculations for quasiparticle properties lead to $\Delta_{e_g}=0.21$ and $\Delta_{t_{2g}}=0.37$ eV,[28] or to a mean value of $\Delta\simeq 0.42$ eV in another case.[29]

Those comparisons show that the qualitative results gained from the many-body ground-state calculations agree very well with experiments and with semiempirical fits to them.[21] The deviations of the LSD calculations should therefore mainly be caused by the apparent inability of the local density functional scheme to deal with anisotropic exchange and correlation effects in the ground state. The estimates done here are clearly not able to include dynamic many-body effects for quasiparticles which should lead to a homogeneous shrinking of the kinetic bands and of the exchange terms as well. Therefore, it is not so astonishing that our estimates lead to splittings for Ni which are somewhat larger than the results of many-body quasiparticle calculations.[28]

The anisotropy for the exchange splittings found for Fe, Co, and Ni should be seen as an upper limit because an additional explicit inclusion of s-d hybridizations is expected to reduce it somewhat.

Although we fully realize all the complications connected with a correct description of the ferromagnetic-paramagnetic transition, it seems to us interesting to relate the values of Curie temperature T_c to the energy difference between the ferromagnetic and paramagnetic states ΔE_{LA}. We use the simplest mean-field approach to a Heisenberg model which gives[30]

$$k_B T_c=\frac{2}{3}\frac{S+1}{S}\Delta E_{\mathrm{LA}}\ , \tag{4.3}$$

where k_B is the Bolzmann constant and S is the spin. Knowing U/W as given above, one finds the energy difference ΔE_{LA} of 0.15, 0.11, and 0.035 eV for Fe, Co, and Ni, respectively (see Tables III–V). Taking $S=1.1$, 0.8, and 0.3 we obtain the Curie temperature of 2200, 1900, and 1150 K. As calculated from the mean-field theory, these Curie temperatures should be by about 30% higher than the exact ones. Taking this into account they compare reasonably well with the experimental values of

1393 and 631 K for Co and Ni, spectively.

The experimental value for I (1043 K) lies still well below the resulting estimate of 600 K. One reason for that overestimate might be tha Eq. (4.3) holds true for completely magnetic systems. F is not completely (80%) ferromagnetic and should there re have a considerably smaller T_c in mean-field theory r eived by (4.3).

One might argue therefore tha T_c can be explained by a complete breakdown of the iti rant ferromagnetic order, in agreement with theories o. Hasegawa[31] and Hubbard[32] who calculated that phase transition in mean-field theory. Certainly smaller corrections due to fluctuations exist. They might be incorporated as done in the work of Korenman and Prange[33] and Capellmann,[34] but should not lead to large ferromagnetic domains.

It should be kept in mind, though, that the model Hamiltonian as well as the above estimate are limited to qualitative and not to really quantitative statements.

V. CONCLUSIONS AND FINAL REMARKS

We have been able to show how correlation effects contribute to magnetic properties in 3*d* metals. Density correlations essentially shift the critical interactions by a constant amount and can be simulated on a one-particle level by renormalized interactions. On the other hand, spin correlations, which take care of exchange effects known as Hund's-rule coupling, add new structures to the phase separation in interaction space. Those spin correlations grow steadily with increasing interaction strength if treated properly within a variational many-body calculation. This contradicts one-particle schemes[19,35] which artificially find a phase transition from no-spin correlations into randomly ordered local moments at a specific interaction strength.

The interaction parameter U has been chosen in such a way for the different ferromagnetic 3*d* metals Fe, Co, and Ni, that the final correlated ferromagnetic ground states had the right magnetic moments. Its values seem to be reasonable (2.4—3.3 eV). The energy differences between correlated paramagnetic and ferromagnetic phase are much smaller than in LSD calculation. Transition temperatures could be estimated from the values found and were roughly in agreement with the experimental ones. Contrary to similar calculation within a LSD scheme spin correlations were present here already in the paramagnetic phase. They lead to energy gains comparable to the ferromagnetic transition itself for Fe. Beyond that the anisotropies in exchange and correlation caused by the simple Hamiltonian used here lead to an improved description of one-particle densities and exchange splittings as compared with the original LSD calculations. Those anisotropies mentioned above are missing in LSD schemes due to its nature, namely the local approximation for the exchange correlation potential.

It should be mentioned finally that the Hund's-rule coupling for Fe and Co causes effective local moments whose squared expectation values $\langle S_l^2 \rangle$ are halfway between the noncorrelated paramagnetic and the correlated ferromagnetic values. It is not astonishing, therefore, that experimentally local magnetic moments can be seen above T_c (Ref. 36) since in addition the energy gain connected with those correlations is of the size of T_c.[4] In the case of Ni there are too few holes available for sizable spin correlations. Here the density correlations directly lead to effective local moments whose squared expectation value is again halfway between the uncorrelated paramagnetic and the correlated ferromagnetic one. That correlation energy gain is again of the size of T_c (Ref. 4) and might so explain local moments above T_c (Ref. 37) as well.

Of course, the phase diagrams of bcc and fcc lattices are by no means complete as we have not discussed any more complicated magnetic states here. Also, there may be quantitative changes of the obtained phase diagrams due to hybridization of *d* and *s* states. We hope that these important problems will be clarified in future work.

ACKNOWLEDGMENTS

We would like to thank Professor P. Fulde for encouraging this work, many stimulating discussions, and a critical reading of the manuscript. It is a pleasure to acknowledge also valuable discussions with Professor O. K. Andersen, Dr. D. Glötzel, Dr. O. Gunnarsson, Dr. P. Horsch, and Dr. P. Thalmeier.

APPENDIX A: RESULTS FOR THE MATRIX ELEMENTS $\langle O_{ln}\tilde{H} \rangle$ AND $\langle O_{ln}\tilde{H}O_{ln'} \rangle$

Here we present the results obtained for the expressions $\langle O_{ln}\tilde{H} \rangle$ and $\langle O_{ln}\tilde{H}\,O_{ln'} \rangle$. They are calculated in the local cluster approximation.

Let us first introduce for convenience

$$p_{i\sigma}=n_{i\sigma}(1-n_{i\sigma})\,, \tag{A1}$$

$$q_{i\sigma}=n_{i\sigma}(1-n_{i-\sigma})\,, \tag{A2}$$

$$a_{i\sigma}=n_{i\sigma}(f_{i\sigma}^{\max}-f_{i\sigma})-(1-n_{i\sigma})f_{i\sigma}\,. \tag{A3}$$

The elements $\langle O_{ln}\tilde{H} \rangle$ contain no contribution from the kinetic energy H_0 since no contraction within the operators O_{ln} is allowed. The results for these elements are

$$\langle O_{li}^{(1)}\tilde{H} \rangle = U_{ii}p_{i\uparrow}p_{i\downarrow}\,, \tag{A4}$$

$$\langle O_{lij}^{(2)}\tilde{H} \rangle = U_{ij}\sum_{\sigma}p_{i\sigma}p_{j-\sigma}+(U_{ij}-J_{ij})\sum_{\sigma}p_{i\sigma}p_{j\sigma}\,, \tag{A5}$$

$$\langle O_{lij}^{(3)}\tilde{H} \rangle = -\tfrac{1}{4}U_{ij}\sum_{\sigma}p_{i\sigma}p_{j-\sigma}+\tfrac{1}{4}(U_{ij}-J_{ij})\sum_{\sigma}p_{i\sigma}p_{j\sigma}-\tfrac{1}{2}J_{ij}\sum_{\sigma}q_{i\sigma}q_{j-\sigma}\,. \tag{A6}$$

The remaining elements may be written as

$$\langle O_{ln}\tilde{H}\ O_{ln'}\rangle=\langle O_{ln}[H_o,\ O_{ln'}]\rangle+\langle O_{ln}\tilde{H}_1 O_{ln'}\rangle\ . \tag{A7}$$

The matrix $\langle O_{ln}\tilde{H}O_{ln'}\rangle$ is symmetric, so we will specify only the elements with $n\leq n'$. The nonvanishing contributions from the kinetic energy are

$$\langle O_{li}^{(1)}[H_0,O_{li}^{(1)}]\rangle=\sum_\sigma p_{i\sigma}a_{i-\sigma}\ , \tag{A8}$$

$$\langle O_{lij}^{(2)}[H_o,O_{lij}^{(2)}]\rangle=(p_{i\uparrow}+p_{i\downarrow})\sum_\sigma a_{j\sigma}+(p_{j\uparrow}+p_{j\downarrow})\sum_\sigma a_{i\sigma}\ , \tag{A9}$$

$$\langle O_{lij}^{(2)}[H_0,O_{lij}^{(3)}]\rangle=\tfrac{1}{4}\sum_\sigma(p_{i\sigma}a_{j\sigma}+p_{j\sigma}a_{i\sigma})-\tfrac{1}{4}\sum_\sigma(p_{i\sigma}a_{j-\sigma}+p_{j\sigma}a_{i-\sigma})\ , \tag{A10}$$

$$\langle O_{lij}^{(3)}[H_0,O_{lij}^{(3)}]\rangle=\tfrac{1}{16}\sum_\sigma(p_{i\sigma}a_{j\sigma}+p_{j\sigma}a_{i\sigma})+\tfrac{5}{16}\sum_\sigma(p_{i\sigma}a_{j-\sigma}+p_{j\sigma}a_{i-\sigma})\ . \tag{A11}$$

The interaction part H_1 (2.3) gives the following elements:

$$\langle O_{li}^{(1)}\tilde{H}_1 O_{li}^{(1)}\rangle=U_{ii}p_{i\uparrow}p_{i\downarrow}(1-2n_{i\uparrow})(1-2n_{i\downarrow})\ , \tag{A12}$$

$$\langle O_{li}^{(1)}\tilde{H}_1 O_{lij}^{(2)}\rangle=(2U_{ij}-J_{ij})p_{i\uparrow}p_{i\downarrow}\sum_\sigma p_{j\sigma}\ , \tag{A13}$$

$$\langle O_{li}^{(1)}\tilde{H}_1 O_{lij}^{(3)}\rangle=\tfrac{1}{4}J_{ij}p_{i\uparrow}p_{i\downarrow}\sum_\sigma(p_{j\sigma}+2q_{j\sigma})\ , \tag{A14}$$

$$\begin{aligned}\langle O_{lij}^{(2)}\tilde{H}_1 O_{lij}^{(2)}\rangle=&(U_{ij}-J_{ij})\sum_\sigma p_{i\sigma}p_{j\sigma}(1-2n_{i\sigma})(1-2n_{j\sigma})\\&+U_{ij}\sum_\sigma p_{i\sigma}p_{j-\sigma}(1-2n_{i\sigma})(1-2n_{j-\sigma})+2U_{ii}p_{i\uparrow}p_{i\downarrow}\sum_\sigma p_{j\sigma}+2U_{jj}p_{j\uparrow}p_{j\downarrow}\sum_\sigma p_{i\sigma}\ ,\end{aligned} \tag{A15}$$

$$\langle O_{lij}^{(2)}\tilde{H}_1 O_{lik}^{(2)}\rangle=(U_{jk}-J_{jk})(p_{i\uparrow}+p_{i\downarrow})\sum_\sigma p_{j\sigma}p_{k\sigma}+U_{jk}(p_{i\uparrow}+p_{i\downarrow})\sum_\sigma p_{j\sigma}p_{k-\sigma}\ , \tag{A16}$$

$$\begin{aligned}\langle O_{lij}^{(2)}\tilde{H}_1 O_{lij}^{(3)}\rangle=&\tfrac{1}{4}(U_{ij}-J_{ij})\sum_\sigma p_{i\sigma}p_{j\sigma}(1-2n_{i\sigma})(1-2n_{j\sigma})-\tfrac{1}{4}U_{ij}\sum_\sigma p_{i\sigma}p_{j-\sigma}(1-2n_{i\sigma})(1-2n_{j-\sigma})\\&+\tfrac{1}{2}J_{ij}\sum_\sigma\{p_{i\sigma}p_{j\sigma}[n_{i-\sigma}(1-n_{j-\sigma})+n_{j-\sigma}(1-n_{i-\sigma})]-p_{i\sigma}p_{j-\sigma}[n_{i-\sigma}n_{j\sigma}+(1-n_{i-\sigma})(1-n_{j\sigma})]\}\ ,\end{aligned} \tag{A17}$$

$$\langle O_{lij}^{(2)}\tilde{H}_1 O_{lik}^{(3)}\rangle=\tfrac{1}{4}(U_{jk}-J_{jk})\sum_\sigma(p_{i\sigma}-p_{i-\sigma})p_{j\sigma}p_{k\sigma}+\tfrac{1}{4}U_{jk}\sum_\sigma(p_{i\sigma}-p_{i-\sigma})p_{j-\sigma}p_{k\sigma}\ , \tag{A18}$$

$$\begin{aligned}\langle O_{lij}^{(3)}\tilde{H}_1 O_{lij}^{(3)}\rangle=&-\tfrac{1}{8}\left[U_{ii}p_{i\uparrow}p_{i\downarrow}\sum_\sigma(p_{j\sigma}+2q_{j\sigma})+U_{jj}p_{j\uparrow}p_{j\downarrow}\sum_\sigma(p_{i\sigma}+2q_{i\sigma})\right]\\&+\tfrac{1}{16}(U_{ij}-J_{ij})\sum_\sigma p_{i\sigma}p_{j\sigma}(1-2n_{i\sigma})(1-2n_{j\sigma})+\tfrac{1}{16}U_{ij}\sum_\sigma p_{i\sigma}p_{j-\sigma}(1-2n_{i\sigma})(1-2n_{j-\sigma})\\&-\tfrac{1}{4}(U_{ij}-J_{ij})\sum_\sigma q_{i\sigma}q_{j-\sigma}[n_{i\sigma}(1-n_{j\sigma})+n_{j-\sigma}(1-n_{i-\sigma})]\\&+\tfrac{1}{4}U_{ij}\sum_\sigma q_{i\sigma}q_{j-\sigma}[n_{i\sigma}n_{j-\sigma}+(1-n_{i-\sigma})(1-n_{j\sigma})]\\&+\tfrac{1}{4}J_{ij}\sum_\sigma\{p_{i\sigma}p_{j\sigma}[(1-n_{i-\sigma})n_{j-\sigma}+n_{i-\sigma}(1-n_{j-\sigma})]+p_{i\sigma}p_{j-\sigma}[n_{i-\sigma}n_{j\sigma}+(1-n_{i-\sigma})(1-n_{j\sigma})]\}\ ,\end{aligned} \tag{A19}$$

$$\langle O_{lij}^{(3)}\tilde{H}_1 O_{lik}^{(3)}\rangle=\tfrac{1}{16}(U_{jk}-J_{jk})(p_{i\uparrow}+p_{i\downarrow})\sum_\sigma p_{j\sigma}p_{k\sigma}-\tfrac{1}{16}U_{jk}(p_{i\uparrow}+p_{i\downarrow})\sum_\sigma p_{j\sigma}p_{k-\sigma}-\tfrac{1}{4}J_{jk}\sum_\sigma q_{i\sigma}q_{j-\sigma}q_{k-\sigma}\ . \tag{A20}$$

APPENDIX B: LOCAL MOMENTS AND FLUCTUATIONS IN THE CORRELATED GROUND STATE

Below we present the method of calculation of local moments and fluctuations in the ground state within the local approach. In such a ground state one finds an average of any operator A_l acting on the site l as follows:

$$\langle A_l\rangle=\langle A_l\rangle_{\mathrm{HFA}}-2\sum_n\eta_n\langle O_{ln}\tilde{A}_l\rangle+\sum_{n,n'}\eta_n\eta_{n'}\langle O_{ln}\tilde{A}_l O_{ln'}\rangle\ , \tag{B1}$$

where $\tilde{A}_l$ contains only the residual part of the two-particle interactions, i.e., its average in the HF state is zero and no contraction within $\tilde{A}_l$ is allowed. Thus the average of any one-particle operator (as for instance the particle number operator n_l or spin S_l^z) does not change in the correlated ground state compared with the HF state.

In what follows we make use of the formula (B1) to find out first how local moments change due to correlation of electrons. As we have found, the second-order terms in η_n's are small and may be neglected, so we will present only the first-order terms here which were used in the calculations discussed in detail in Sec. IV. They were calculated according to the same scheme as those used to calculate the correlation energy (see Sec. II and Appendix A).

A local moment in a given i state and in the HFA is

$$\langle \vec{S}_{li}^{\,2} \rangle_{\mathrm{HFA}} = \tfrac{3}{4} \sum_{\sigma} n_{i\sigma}(1-n_{i\sigma}) , \tag{B2}$$

and obviously depends on U/W only through the actual occupations $n_{i\sigma}$. The only nonvanishing first-order element $\langle O_{ln} \vec{S}_{li}^{\,2} \rangle$ which changes its value in the correlated state is

$$\langle O_{li}^{(1)} \vec{S}_{li}^{\,2} \rangle = -\tfrac{1}{2} n_{i\uparrow} n_{i\downarrow}(1-n_{i\uparrow})(1-n_{i\downarrow}) . \tag{B3}$$

It describes gradual formation of the local moment with increasing U/W, as seen in Figs. 4, 7, and 9, and vanishes in the CF state, where the HFA becomes exact for $\langle \vec{S}_{li}^{\,2} \rangle$.

A total moment at a site l is composed in the HFA of five uncoupled local moments of different states i and, if the state is ferromagnetic, from the respective contribution coming from the zth components of the spins $\vec{S}_{li}$,

$$\langle \vec{S}_l \rangle_{\mathrm{HFA}} = \tfrac{3}{4} \sum_{i,\sigma} n_{i\sigma}(1-n_{i-\sigma}) + \tfrac{1}{2} \sum_{\substack{i,j \\ i \neq j}} (n_{i\uparrow}-n_{i\downarrow})(n_{j\uparrow}-n_{j\downarrow}) , \tag{B4}$$

where the second sum runs over different pairs of $\{i,j\}$. In the correlated state we find the following matrix elements:

$$\langle O_{li}^{(1)} \vec{S}_l \rangle = -\tfrac{3}{2} n_{i\uparrow} n_{i\downarrow}(1-n_{i\uparrow})(1-n_{i\downarrow}) , \tag{B5}$$

$$\langle O_{lij}^{(2)} \vec{S}_l \rangle = \tfrac{1}{2} \sum_{\sigma} n_{i\sigma}(1-n_{i\sigma}) n_{j\sigma}(1-n_{j\sigma}) - \tfrac{1}{2} \sum_{\sigma} n_{i\sigma}(1-n_{i\sigma}) n_{j-\sigma}(1-n_{j-\sigma}) , \tag{B6}$$

$$\langle O_{lij}^{(3)} \vec{S}_l \rangle = \tfrac{1}{2} \sum_{\sigma} n_{i\sigma}(1-n_{i-\sigma}) n_{j-\sigma}(1-n_{j\sigma}) + \tfrac{1}{8} \sum_{\sigma} n_{i\sigma}(1-n_{i\sigma}) \sum_{\sigma'} n_{j\sigma'}(1-n_{j\sigma'}) , \tag{B7}$$

which were used to calculate the moment according to Eq. (B1).

Other quantities which were calculated to demonstrate correlation effects within d electrons were charge and spin fluctuations (4.1)–(4.2). In the HFA, when the electrons are treated as independent, we have

$$\sigma^2_{\mathrm{HFA}}(n_l) = n - \sum_{i,\sigma} n_{i\sigma}^2 , \tag{B8}$$

$$\sigma^2_{\mathrm{HFA}}(S_l^z) = \tfrac{1}{4} \sum_{i,\sigma} n_{i\sigma}(1-n_{i\sigma}) = \tfrac{1}{4} \sigma^2_{\mathrm{HFA}}(n_l) . \tag{B9}$$

The corrections in the correlated state are due to the quantities $\langle n_l^2 \rangle$ and $\langle (S_l^z)^2 \rangle$ in Eqs. (4.1) and (4.2). The respective matrix elements needed to find those corrections are

$$\langle O_{li}^{(1)} n_l^2 \rangle = 2 n_{i\uparrow} n_{i\downarrow}(1-n_{i\uparrow})(1-n_{i\downarrow}) , \tag{B10}$$

$$\langle O_{lij}^{(2)} n_l^2 \rangle = 2 \sum_{\sigma} n_{i\sigma}(1-n_{i\sigma}) \sum_{\sigma'} n_{j\sigma'}(1-n_{j\sigma'}) , \tag{B11}$$

$$\langle O_{lij}^{(3)} n_l^2 \rangle = \tfrac{1}{2} \sum_{\sigma} n_{i\sigma}(1-n_{i\sigma}) n_{j\sigma}(1-n_{j\sigma}) - \tfrac{1}{2} \sum_{\sigma} n_{i\sigma}(1-n_{i\sigma}) n_{j-\sigma}(1-n_{j-\sigma}) , \tag{B12}$$

$$\langle O_{li}^{(1)} (S_l^z)^2 \rangle = -\tfrac{1}{2} n_{i\uparrow} n_{i\downarrow}(1-n_{i\uparrow})(1-n_{i\downarrow}) , \tag{B13}$$

$$\langle O_{lij}^{(2)} (S_l^z)^2 \rangle = \langle O_{lij}^{(3)} n_l^2 \rangle , \tag{B14}$$

$$\langle O_{lij}^{(3)} (S_l^z)^2 \rangle = \tfrac{1}{8} \sum_{\sigma} n_{i\sigma}(1-n_{i\sigma}) \sum_{\sigma'} n_{j\sigma'}(1-n_{j\sigma'}) . \tag{B15}$$

---

*On leave of absence from the Institute of Physics, Jagellonian University, Cracow, Poland.

[1]For a review, see J. Callaway, in *Physics of Transition Metals, 1980,* edited by P. Rhodes (IOP, London, 1980), p. 1.

[2]O. Gunnarsson, J. Phys. F 6, 587 (1976).

[3]A. M. Oleś, Phys. Rev. B 23, 271 (1981).

[4]G. Stollhoff and P. Thalmeier, Z. Phys. B 43, 13 (1981).

[5]O. K. Andersen, Phys. Rev. B 12, 3060 (1975).

[6]For a review of the Stoner theory, see E. P. Wohlfarth, in *Physics of Transition Metals, 1980,* edited by P. Rhodes (IOP, London, 1980), p. 161.

[7]G. Stollhoff and P. Fulde, Z. Phys. B 26, 257 (1977); 29, 231 (19781).

[8]G. Stollhoff and P. Fulde, J. Chem. Phys. 73, 4548 (1980).

[9]M. C. Gutzwiller, Phys. Rev. A 137, 1726 (1965).

[10]O. K. Andersen and O. Jepsen, Physica (Utrecht) B91, 317 (1977).

[11]D. Glötzel, O. K. Andersen, and O. Jepsen (unpublished).

[12]P. Thalmeier and L. M. Falicov, Phys. Rev. B 20, 4637 (1979).

[13]M. Tinkham, *Group Theory and Quantum Mechanics* (McGraw-Hill, New York, 1964), p. 174.

[14]L. Kleinman and K. Mednick, Phys. Rev. B 24, 6880 (1981).

[15]A. M. Oleś, Phys. Rev. B 28, 327 (1983).

[16]J. Friedel and C. M. Sayers, J. Phys. (Paris) 38, 697 (1977).

[17]P. Horsch and P. Fulde, Z. Phys. B 36, 23 (1979).

[18]G. Treglia, F. Ducastelle, and D. Spanjaard, J. Phys. (Paris) 41, 281 (1980).

[19]V. Heine, J. H. Samson, and G. M. M. Nex, J. Phys. F 11, 2645 (1981).

[20]V. L. Moruzzi, J. F. Janak, and A. R. Williams, *Calculated Electronic Properties of Metals* (Pergamon, New York, 1978).

[21]J. F. Cooke, J. W. Lynn, and H. L. Davis, Phys. Rev. B 21,

4118 (1980).
[22]G. Treglia, F. Ducastelle, and D. Spanjaard, J. Phys. (Paris) 43, 341 (1982).
[23]B. N. Cox, M. A. Coulthard, and P. Lloyd, J. Phys. F 4, 807 (1974).
[24]H. J. F. Jansen, G. G. Lonzarich, and F. M. Mueller, *Physics of Transition Metals 1980,* edited by P. Rhodes (IOP, London, 1980), p. 191.
[25]D. E. Eastman, F. J. Himpsel, and J. A. Knapp, Phys. Rev. Lett. 44, 95 (1980).
[26]E. Dietz, U. Gerhardt, and C. J. Maeta, Phys. Rev. Lett. 40, 892 (1978).
[27]W. Eberhardt and E. W. Plummer, Phys. Rev. B 21, 3245 (1980).
[28]A. Liebsch, Phys. Rev. Lett. 43, 1431 (1979).
[29]L. Kleinmann, Phys. Rev. B 19, 1295 (1979).
[30]See for instance, D. Wagner, *Einführung in die Theorie des Magnetismus* (Vieweg, Braunschweig, 1966).
[31]H. Hasegawa, in *Physics of Transition Metals, 1980,* edited by P. Rhodes (IOP, London, 1980), p. 209.
[32]J. Hubbard, Phys. Rev. B 19, 2626 (1979); 20, 4548 (1980).
[33]V. Korenman, J. L. Murray, and R. E. Prange, Phys. Rev. B 16, 4032 (1977).
[34]H. Capellmann, J. Phys. F 4, 1966 (1974); Z. Phys. B 34, 29 (1979).
[35]D. R. Penn, Phys. Rev. 142, 350 (1966).
[36]J. W. Lynn, Phys. Rev. B 11, 2624 (1975).
[37]H. A. Mook, J. W. Lynn, and R. M. Nicklow, Phys. Rev. Lett. 30, 556 (1973).